Available online at www.sciencedirect.com

SCIENCE DIRECT®

Physics Letters A 356 (2006) 1–7

PHYSICS LETTERS A

www.elsevier.com/locate/pla

Conjugacy classes and chiral doublets in the Hénon Hamiltonian repeller

Antônio Endler, Jason A.C. Gallas *

Instituto de Física, Universidade Federal do Rio Grande do Sul, 91501-970 Porto Alegre, Brazil

Received 6 April 2006; accepted 18 April 2006

Available online 2 May 2006

Communicated by A.R. Bishop

Abstract

Conjugacy classes hidden behind orbital symmetries under reflection are brought to light through the recognition of the fundamental role played by certain algebraic clusters underlying orbital equations of the area-preserving Hénon map, a discrete proxy of open Hamiltonian systems that exhibit chaotic scattering and transport. Specific number-fields ruling orbital coordinates are shown to slave large sets of orbits into being necessarily nonlinearly coupled. Particularly remarkable is the conjugacy class characterized by non-self-symmetric chiral doublets which completely dominates at higher periods.

1. Introduction

A long-outstanding problem in classical mechanics and statistical physics, with far-reaching and important applications in several areas, is that connected with studying symmetries and asymmetries of periodic motions in phase-space. This problem was and still is one of the central problems and active fields of research in Celestial Mechanics as emphasized in very recent investigations of motions in planetary and satellite systems [1–4]. Apart from these technologically important applications, the study of symmetries and orbits in area- and orientation-preserving maps has also helped to clarify intricate dynamical processes like, for example, the emergence of infinitely many symmetric periodic orbits through saddle-node or equiperiod bifurcation [5] and the dynamics of open conservative systems, i.e., conservative systems having unbounded phase-space as, e.g., "leaking" Hamiltonian systems [6].

Here we study orbital symmetries and asymmetries computed analytically and systematically for the Hamiltonian (area-preserving) $b=-1$ limit of the Hénon map

$$x_{t+1} = a - x_t^2 + bx_{t-1}. \tag{1}$$

This map is a well-known discrete proxy of open Hamiltonian systems that exhibit chaotic scattering and transport [7]. It was found very early to reproduce experimental results involving ferromagnetic resonance in yttrium iron garnet [8].

Our key result is the discovery of a natural segregation of orbits into three *conjugacy* classes when one considers orbital symmetries with respect to a reflection in phase-space about the $y=x$ symmetry line, as defined in Table 4. As we argue below, under such reflection every periodic orbit (cycle) falls into one of three possible classes:

- $\mathcal{D}$: *diagonal cycles*: self-conjugate periodic orbits with points on the diagonal, as illustrated in Fig. 1 below.
- $\mathcal{N}$: *non-diagonal cycles*: self-conjugate periodic orbits without points on the diagonal, shown in Fig. 1 below.
- $\mathcal{C}$: *chiral doublets*: pairs of non-self-conjugate cycles that map into each other, illustrated in Figs. 2–4 below.

This classification is independent of the control parameter a. Orbits are specially interesting for $a > a_h$, where $a_h \simeq 5.69931\ldots$, since beyond this value there is a complete Smale horseshoe [9] and all orbits are real.

Formally, the conjugacy classes are defined by the three factors composing Eq. (5). The next section explains this equation and presents a methodology which allows factors to be computed systematically for arbitrary period.

* Corresponding author.
E-mail addresses: aendler@if.ufrgs.br (A. Endler), jgallas@if.ufrgs.br (J.A.C. Gallas).

0375-9601/$ – see front matter
doi:10.1016/j.physleta.2006.04.042

2. The polynomials $\mathbf{P}_k(x)$ and $\mathbf{S}_k(\sigma)$

It is always possible to reduce the problem of finding the periodic orbits of dynamical systems of algebraic origin of any dimension to the much simpler problem of finding the roots of a fundamental pair of *univariate* polynomials, say,

$$\mathbf{P}_k(x) \quad \text{and} \quad \mathbf{S}_k(\sigma), \tag{2}$$

indexed by the orbital period k and involving only the physical parameters of the model [10–12]. This pair of polynomials provides exact analytical expressions encoding *simultaneously* all k-periodic orbits as a function of the sum σ of orbital points. We now summarize briefly the procedure employed to obtain the polynomials explicitly. The general procedure was introduced in Ref. [10] and applied in Refs. [11,12]. The generic origin of periodicity is discussed in Ref. [13].

First, from Eq. (1) note that a generic period-k orbit is defined by a set $\{x_\ell\}$ of numbers containing k *coordinates* x_ℓ of the orbit, which for convenience we label from $\ell = 1$ to $\ell = k$. These k coordinates may be used to construct a polynomial of degree k defining the orbit

$$\mathbf{P}_k(x) = \prod_{\ell=1}^{k}(x - x_\ell). \tag{3}$$

Now, recall a basic text-book result about the relation between roots and coefficients of polynomials: in any polynomial of degree k, the negative of the coefficient of the term of degree $k-1$ is the elementary symmetric function representing the *sum* of all roots, in our case, the sum of all orbital coordinates x_ℓ. We call this sum σ and, by eliminations with the help of Eq. (1), express all other coefficients of x in $\mathbf{P}_k(x)$ as functions of σ. After all eliminations $\mathbf{P}_k(x)$ is a polynomial involving three quantities only: x, σ and the control parameter a. For explicit examples, see Eqs. (6), (15) and (16).

The process of replacing all coefficients of $\mathbf{P}_k(x)$ by functions of σ produces an important additional polynomial, a *constraint equation* for σ, denoted by

$$\mathbf{S}_k(\sigma) = 0. \tag{4}$$

This polynomial involves only σ and the parameters of the model, a in the present case. For explicit examples, see Table 1 and, more generically, Eq. (5). The roots σ_ℓ of Eq. (4) are the numerical values of σ needed in the corresponding polynomial $\mathbf{P}_k(x)$ to fix each individual orbit.

Table 1
The factors composing $\mathbf{S}_k(\sigma)$ and defining the two classes of self-symmetric orbits, the only classes which exist for periods $k \leqslant 5$. The factors are valid for arbitrary values of a

k	$\mathbf{S}_k(\sigma)$
1	$D_1(\sigma) = \sigma^2 + 2\sigma - a$
2	$N_2(\sigma) = \sigma - 2$
3	$D_3(\sigma) = \sigma^2 - 2\sigma + 2 - a$
4	$D_4(\sigma) = \sigma$, $N_4(\sigma) = \sigma^2 - 4a$
5	$D_5(\sigma) = \sigma^6 - 2\sigma^5 - (11a + 12)\sigma^4 + 12(2 + 3a)\sigma^3$ $+ (20a + 36 + 19a^2)\sigma^2 - 2(a + 6)(17a + 2)\sigma - 9a^3$ $+ 88a^2 + 56 + 28a$

We remark that our choice of expressing all coefficients of $\mathbf{P}_k(x)$ as functions of the sum σ of orbital points is motivated by the interpretation of σ as a sort of *mean-field* signature of each individual orbit. As pointed out in Ref. [10], any coefficient of $\mathbf{P}_k(x)$ could be used to represent all remaining coefficients equally well, since all coefficients are interconnected by the well-known *elementary symmetric functions* considered first by Girard and by Newton [14], constructed with the roots of $\mathbf{P}_k(x)$. Two particularly fruitful parameterizations are σ, the sum of the orbital points, and π, their product. Here we focus only on σ.

In the next section we show that $\mathbf{S}_k(\sigma)$ is formed by certain characteristic factors and discuss their distinct nature. As indicated in Table 1, up to period $k = 5$ the polynomial $\mathbf{S}_k(\sigma)$ contains only two types of factors, namely $D_k(\sigma)$ and $N_k(\sigma)$. The meaning of this notation is also explained in the next section.

3. The factors C_k, D_k, N_k and the classes

The purpose of this section is to show that the polynomials $\mathbf{S}_k(\sigma)$ of Eq. (4) emerge automatically decomposed into three factors, namely,

$$\mathbf{S}_k(\sigma) = C_k^2(\sigma) D_k(\sigma) N_k(\sigma), \tag{5}$$

and that these factors are the mathematical objects characterizing the clusters responsible for the three algebraic conjugacy classes. The fact that the roots σ_ℓ originating from each cluster are number-theoretically conjugate quantities justifies the name *conjugacy* classes. From an algebraic point of view, this conjugacy is the key theoretical novelty. It implies strong orbital correlations and interdependencies.

To fix ideas, consider the problem of determining explicitly the exact analytical expressions for all possible orbits of period $k = 4$ of the Hénon map, Eq. (1). The solution of this problem is trivial because Ref. [10] contains the solution for arbitrary a and b. Substituting $b = -1$ in the general expressions one obtains the polynomial $\mathbf{P}_4(x) = \mathbf{P}_4(x, \sigma)$ which, through the parameter σ, encodes simultaneously all possible period-4 orbits:

$$\begin{aligned}\mathbf{P}_4(x) = {} & x^4 - \sigma x^3 + \left(\sigma^2 + 2\sigma - 4a\right)x^2/2 \\ & - \left(\sigma^2 + 6\sigma - 10a\right)\sigma x/6 + \sigma^4/24 \\ & + \sigma^3/2 - 2a\sigma^2/3 + a^2 - a\sigma.\end{aligned} \tag{6}$$

In the present case [10], σ is a root of the cubic

$$\mathbf{S}_4(\sigma) = \sigma\left(\sigma^2 - 4a\right). \tag{7}$$

The degree of $\mathbf{S}_4(\sigma)$ tells that Eq. (1) contains altogether three period-4 orbits, one for each root of $\mathbf{S}_4(\sigma)$, namely $-2\mathfrak{r}, 0, 2\mathfrak{r}$, where $\mathfrak{r} = \sqrt{a}$. When substituted into $\mathbf{P}_4(x)$, these roots generate three orbits, respectively,

$$P_{4,1}(x) = \left(x^2 - a - 2\mathfrak{r}\right)(x + \mathfrak{r})^2, \tag{8}$$

$$P_{4,3}(x) = x^4 - 2ax^2 + a^2 = \left(x^2 - a\right)^2, \tag{9}$$

$$P_{4,7}(x) = \left(x^2 - a + 2\mathfrak{r}\right)(x - \mathfrak{r})^2. \tag{10}$$

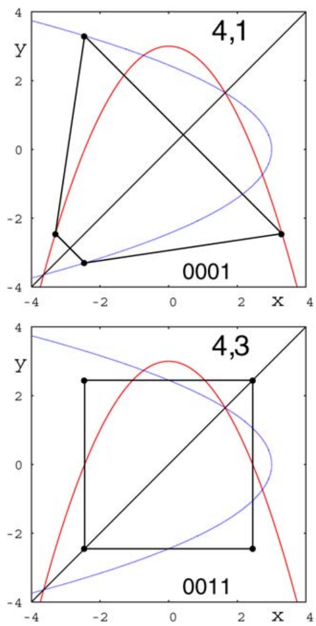

Fig. 1. The two distinct classes of orbits self-symmetric under reflection about the symmetry diagonal $y = x$, here of period four and for $a = 6$ (complete Smale horseshoe). Orbits 4,1 and 4,7 are of class $\mathcal{N}$: have no points on the diagonal. Orbit 4,3 is of class $\mathcal{D}$: has points on the diagonal.

These orbits are shown in Fig. 1 for $a = 6$, the smallest integer where a complete Smale horseshoe exists [12]. All three orbits in Fig. 1 are clearly *self-symmetric* under reflection about the $y = x$ symmetry diagonal and come in two flavors: with or without points on the axis. Obviously, self-symmetric orbits with even periods k cannot have an odd number of points on the diagonal. Self-symmetric orbits may have points on the symmetry diagonal or on the time-reversal symmetry parabolas shown in the figure.

Self-symmetric orbits are the only ones observed up to period 5 and Table 1 summarizes the specific expressions $\mathbf{S}_k(\sigma)$ for $k \leqslant 5$. The simple two-factor structure of $\mathbf{S}_k(\sigma)$ found for periods $k \leqslant 5$ changes when $k \geqslant 6$ by the appearance of an additional factor, $C_k(\sigma)$, containing all chiral doublets, as we now show.

For arbitrary values of a explicit calculations show that there are nine period-6 orbits and that

$$\mathbf{S}_6(\sigma) = C_6^2(\sigma) D_6(\sigma) N_6(\sigma), \tag{11}$$

where

$$C_6(\sigma) = \sigma - 2, \tag{12}$$

$$D_6(\sigma) = \sigma^2 + 4\sigma - 4a, \tag{13}$$

$$N_6(\sigma) = \sigma^5 + 2\sigma^4 - 4(5a+4)\sigma^3 + 8\sigma^2 a + 4\big(16a^2 + 12a + 9\big)\sigma + 128a^2 - 96a + 72. \tag{14}$$

As before for $\mathbf{P}_4(x)$, in the Hamiltonian case ($b = -1$) and for $\sigma = 2$ a general expression available in the literature [11] simplifies to

$$\mathbf{P}_6(x) = \big[x^3 - (1+\mathfrak{r})x^2 - ax + a(1+\mathfrak{r}) - 1\big] \times \big[x^3 - (1-\mathfrak{r})x^2 - ax + a(1-\mathfrak{r}) - 1\big], \tag{15}$$

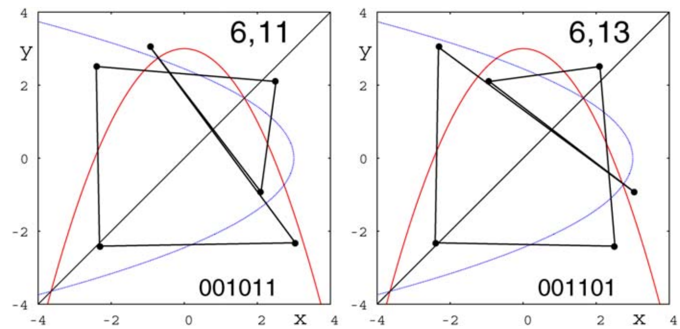

Fig. 2. The chiral doublet of period 6 defined by the roots of Eq. (15), here for $a = 6$. Numbers refer to the usual binary labeling (shown on the bottom) and decimal equivalent (top). These orbits are non-self-symmetric: under reflection about the symmetry line $y = x$ they map into each other. Chiral orbits may never contain points on the time-reversal symmetry parabolas or on the symmetry line $y = x$ because the transformation $(x, y) \mapsto (y, x)$ must send one orbit into the other.

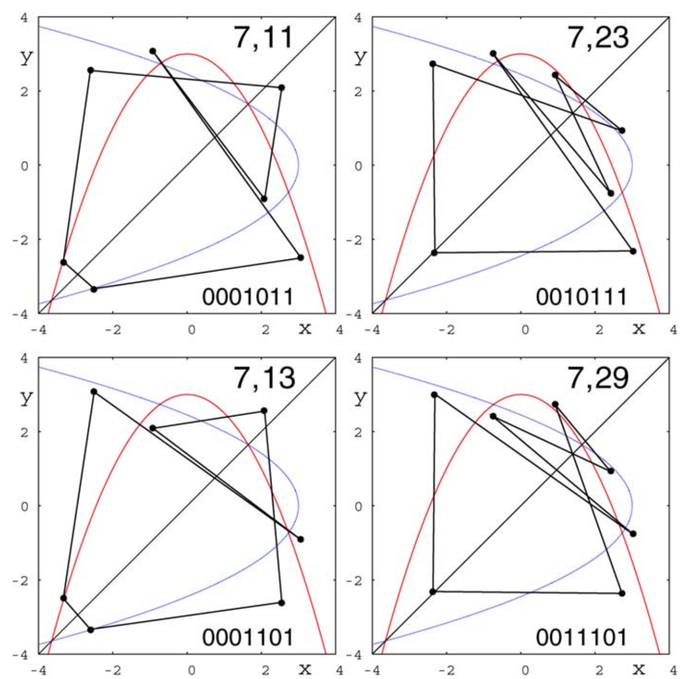

Fig. 3. The two chiral doublets of period 7 for $a = 6$. Under reflection about the $y = x$ diagonal the orbits 7,11 and 7,23 map into their partners 7,13 and 7,29, and vice versa.

where $\mathfrak{r} = \sqrt{a-3}$ is the relative-quadratic irrationality breaking the sextic generically. A pitchfork bifurcation occurs for $a = 3$, when a stable class $\mathcal{D}$ orbit looses stability in favor of a chiral doublet, stable for $3 < a < 3.00795\ldots$. The roots of Eq. (15) define the coordinates of the chiral doublet shown in Fig. 2. Individual orbits are obtained by selecting the proper inphase combination of roots needed to start iterating Eq. (1). The stability of the doublet is ruled by degenerate σ values, identical for both orbits. Thus, chiral doublets are always both stable or both unstable, depending on a. The factors $C_k(\sigma)$ of $\mathbf{S}_k(\sigma)$ define the specific values of σ leading to chiral doublets.

Analogously, for period 7 we compute all 18 orbits and a decomposition $\mathbf{S}_7(\sigma) = C_7^2(\sigma) D_7(\sigma)$ where $D_7(\sigma)$ is a polynomial of degree 14 and $C_7(\sigma) = \sigma^2 - 2\sigma - a$. Thus, there are

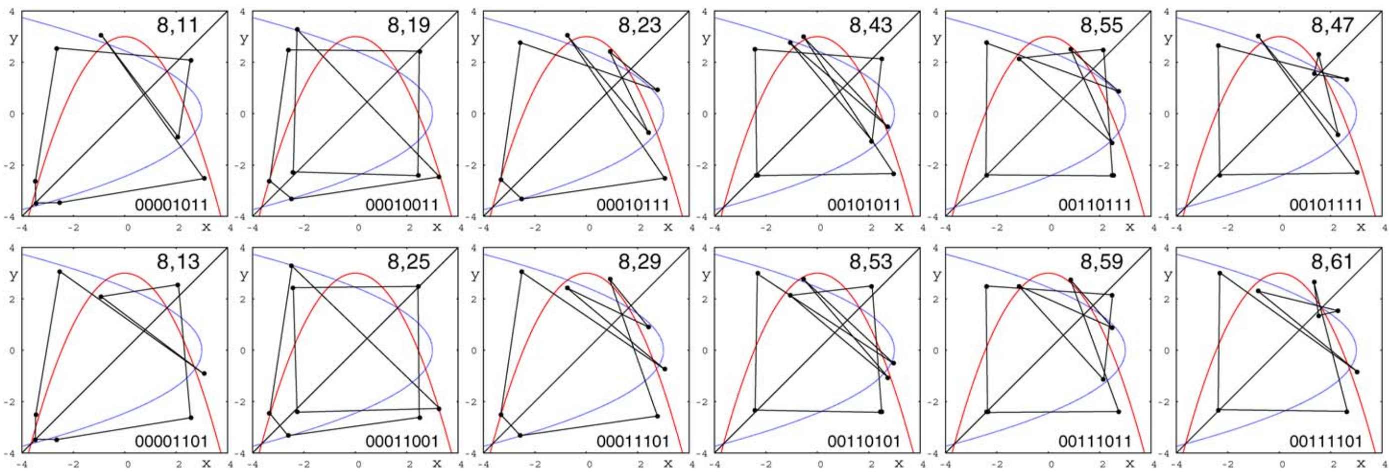

Fig. 4. The six non-self-symmetric period-8 chiral duos defined by the roots of Eq. (A.2) in Appendix A. Proper in-phase initial points are given in Table 4 in Appendix A. Note the conspicuous presence and evolution of the doublets with the same labels and similar shapes as those in Figs. 2 and 3. The sum σ of the orbital coordinates increases from left to right (see Table 4). Points of chiral orbits may never lie on the symmetry diagonal or on the time-reversal symmetry parabolas. Note the inner reflection symmetries of conjugate binary labels.

two chiral doublets and 14 self-symmetric orbits with points on the diagonal. The roots σ_ℓ of $C_7(\sigma)$ generate a pair of chiral doublets when substituted in

$$\begin{aligned}\bar{P}_7(x) = {} & x^7 - \sigma x^6 - (3a - 2\sigma)x^5 - \big(2a - (3a-4)\sigma - 4\big)x^4 \\ & + \big(3a^2 - 2(2a-1)\sigma + 1\big)x^3 \\ & + \big(4a^2 - 10a - \big(3a^2 - 8a + 1\big)\sigma - 2\big)x^2 \\ & - (a-1)\big(a^2 - 2a\sigma + a + 2\big)x \\ & - 2a^3 + 6a^2 + 2a + 3\big(a^3 - 4a^2 + a - 2\big)\sigma. \end{aligned} \tag{16}$$

One doublet is obtained for

$$\sigma_{7,11} = \sigma_{7,13} = 1 + \sqrt{a+1}, \tag{17}$$

while the conjugate doublet follows from the conjugate σ, namely,

$$\sigma_{7,23} = \sigma_{7,29} = 1 - \sqrt{a+1}. \tag{18}$$

Fig. 3 shows the orbits composing the period-7 doublets. Note that all four orbits are compactly encoded by σ in a single polynomial.

For period 8 we obtain the decomposition $\mathbf{S}_8(\sigma) = C_8^2(\sigma) \times D_8(\sigma) N_8(\sigma)$, defining 6 orbits of class $\mathcal{D}$, 12 of class $\mathcal{N}$, and 6 chiral doublets defined by

$$\begin{aligned} C_8(\sigma) = {} & \sigma^6 - 4\sigma^5 - 4(2a+1)\sigma^4 + 16(2a+1)\sigma^3 \\ & + 16a(a+1)\sigma^2 - 64a(a+1)\sigma - 16. \end{aligned} \tag{19}$$

The polynomial $\mathbf{W}_8(x)$ encoding simultaneously all period-8 doublets is given in Appendix A.

Fig. 4 shows the six period-8 doublets, two of them similar to those in Fig. 3 but with an extra orbital point. Of course, there are also period-8 orbits of class $\mathcal{D}$ and $\mathcal{N}$, but the polynomials defining them are too big to be listed here.

The systematic seems now well-established and was corroborated by computing with ad hoc computer algebra routines all pairs $\mathbf{P}_k(x)$ and $\mathbf{S}_k(\sigma)$ up to period $k = 20$. Again, and for arbitrary values of the control parameter a, $\mathbf{S}_k(\sigma)$ always decomposes systematically as represented in Eq. (5). The specific number of orbits found in each class is summarized for $k \leqslant 20$ in Table 2.

Table 2
Partitions of the total number M_k of period-k orbits, defined in Eq. (20), into the number of orbits composing each class. The rightmost column shows the percentage of chiral orbits

k	M_k	C_k	D_k	N_k	%
1	2	0	2	0	0
2	1	0	0	1	0
3	2	0	2	0	0
4	3	0	1	2	0
5	6	0	6	0	0
6	9	2×1	2	5	22.2
7	18	2×2	14	0	22.2
8	30	2×6	6	12	40.0
9	56	2×14	28	0	50.0
10	99	2×30	12	27	60.6
11	186	2×62	62	0	66.7
12	335	2×127	27	54	75.8
13	630	2×252	126	0	80.0
14	1161	2×500	56	119	84.9
15	2182	2×968	246	0	88.7
16	4080	2×1860	120	240	91.2
17	7710	2×3600	510	0	93.4
18	14532	2×6902	238	490	95.0
19	27594	2×13286	1022	0	96.3
20	52377	2×25446	495	990	97.2

From the results above one sees that the roots of the factors C_k, D_k, N_k of $\mathbf{S}_k(\sigma)$ define the orbits in each class, C standing for chiral, D for diagonal and N for non-diagonal orbits. Symmetry under reflection about the $y = x$ diagonal forbids the existence of class $\mathcal{N}$ for odd k, i.e., $N_k(\sigma) \equiv 1$ for odd k. Symmetry also imposes that for even (odd) periods class $\mathcal{D}$ orbits will have an even (odd) number of points on the diagonal. We can find no reason for the classes not to remain well-defined as the period further grows. The specific number-fields (base fields) defined by the σ-factors in Eq. (5)

are the strong links slaving orbits into clusters and sums of orbital points into classes.

It is known that in the limit in which all possible horseshoe orbits exist, binary Smale horseshoe labels are useful because they assign a unique name to each periodic point and facilitate counting cycles. For instance, the number M_k of cycles of period k is related to the 2^k cycle points by the Möbius inversion formula

$$M_k = \frac{1}{k}\sum_{d|k}\mu(k/d)2^d, \tag{20}$$

where $\mu(n)$ is the Möbius function [15], and the sum runs over all divisors d of k. Table 2 summarizes the partition of the M_k orbits as obtained by computing all of them explicitly. For prime k there are $2^{(k+1)/2} - 2$ orbits of class $\mathcal{D}$. The partition of M_k into the number of orbits in each class is a nice challenge in combinatorial analysis.

The decomposition summarized by Eq. (5) and the overwhelming abundance of "handedness" manifest in Table 2 are our main theoretical results. They are both independent of the numerical value of the control parameter a. The remarkably strong dominance of chiral (asymmetric) orbits seen in Table 2 as the period grows contrasts sharply with recent remarkable findings concerning the signature of time-reversal symmetry of polynomial automorphisms over finite fields, an exceptional context where symmetric orbits dominate statistics over asymmetric ones [16].

4. Final comments

The investigation of conservative dynamical systems with two degrees of freedom has a long history [17–24]. Birkhoff [18,19] observed that conservative dynamical systems with two degrees of freedom may be decomposed generically into a pair of involutions. These involutions were first exploited by de Vogelaere [20]. For instance, the reversing involution, or *reversor*, $\mathbf{R}(x, y) = (y, x)$, may be conveniently used to segregate orbits into two broad classes: symmetric and non-symmetric orbits. Until now the emphasis has been by far in the study of symmetric orbits, the easiest ones to find numerically. But non-symmetric orbits have been also occasionally mentioned in the literature, mostly rather briefly. For instance, after summarizing de Vogelaere's classification [20] of symmetric periodic orbits based on the involution $\mathbf{R}$, Devaney [21] remarks on p. 96 that "The remaining [orbits] are called *non-symmetric*. They always occur in pairs $\boldsymbol{\gamma}$ and $\mathbf{R}(\boldsymbol{\gamma})$." A whole section dedicated to asymmetric orbits appears in the very nice paper by Jiménez-Lara and Piña [23] dealing with Störmer's problem, namely the problem of finding the orbits for an electric charge in a magnetic dipole field [25].

The general non-self-symmetric involutions and chirality (mirror symmetry of non-self-symmetric orbital pairs) discussed here do not seem to have been observed before.[1] These involutions are different from the popular involutions normally connected with time-reversal symmetries and should not be confused with them. The connection between involutions and factorizations is the subject of a separate work [29]. Generically, factorization is a very rare event in algebraic geometry and in this sense the orbital segregation summarized by Eq. (5) is rather surprising.

Concerning generality, we recall a result of Friedland and Milnor stating that every polynomial automorphism that is not dynamically trivial is conjugate to a composition of generalized Hénon transformations [30]. Thus, we believe that the results reported here could be also valid for physical systems ruled by rational equations of motion, polynomials in particular. This, however, remains to be investigated more closely. The study of planar polynomial automorphisms whose inverse is also a polynomial map, the situation discussed here, is of great interest for applications in physics since reversibility is frequently associated with Hamiltonian systems and, more generally, to conservative dynamics. Another interesting open question is the possible application of the algebraic conjugacy of orbits to the effective computation of the topological entropy, to assess the complexity of Hénon and Hénon-like systems along the lines of recent works [31–33].

From a physical point of view, Eq. (5) may be regarded as implying two different levels of orbital organization. First, there is a sort of coarse-grained macroscopic upper level of orbital organization manifest by the decomposition of $\mathbf{S}_k(\sigma)$ into the classes $\mathcal{C}$, $\mathcal{D}$, and $\mathcal{N}$. Then, underlying each individual class there is a microscopic level responsible for the selection of highly symmetric number-field conjugacies and very delicate balance between them, manifest in the coordinates of orbital points of individual orbit. This latter level is the lowest level possible from a mathematical point of view: it is the "atomic" number-theoretic level responsible for exquisite symmetries and conjugacies between the *individual numbers* defining orbital coordinates.

So far, symmetric orbits have overwhelmingly dominated attention in the literature. From Table 2 it is possible to get the impression that the rarity of asymmetric orbits at low periods could explain their relative oblivion. This work contributes to reestablish the balance by shedding light on the crowded sets of asymmetric orbits, by far the dominating class of orbits at higher periods. At any rate, symmetric orbits are extremely useful but quite exceptional.

Acknowledgements

The authors are grateful to M.A.M. de Aguiar, C.A. Buzzi, R.L. Devaney, M. Haase, M. Hénon, J.S.W. Lamb, J.D. Meiss, C. Mira, C. Simó, T. Tél and F. Vivaldi for enlightening email exchanges. A.E. thanks Conselho Nacional de Desenvolvimento Científico e Tecnológico (CNPq), Brazil, for a doctoral fellowship. J.A.C.G. thanks CNPq for a senior research fellowship.

[1] We are indebted to C. Mira for kindly pointing out that our involutions may be described in a generic *symbolic plane* with the help of the one-dimensional quadratic map, as done in Section 6.6.2 of his book [26]. See also work by Kawakami [27,28].

Appendix A

This appendix records the polynomial *cluster* defining the exact orbital coordinates simultaneously for all six chiral doublets in Fig. 4. This polynomial results from straightforward but very long computations and is given in Table 3. It contains many number-theoretical features, in particular it is composed by relatively big primes.

For arbitrary values of a, the 12 period-8 chiral orbits are entangled among the roots of the following polynomial cluster

$$\begin{aligned}\mathbf{W}_8(x) = {} & x^{48} - 4x^{47} - 12(2a-1)x^{46} + 4(23a-2)x^{45} \\ & + 6\big(46a^2 - 48a - 3\big)x^{44} - 4\big(253a^2 - 60a - 27\big)x^{43} \\ & - 4\big(506a^3 - 825a^2 - 43a + 34\big)x^{42} \\ & + 4\big(1771a^3 - 798a^2 - 519a + 21\big)x^{41} + \cdots \\ & + 4\big(a^{20} - 18a^{19} + 117a^{18} - 267a^{17} - 394a^{16} \\ & + 3017a^{15} - 4328a^{14} - 1634a^{13} + 8228a^{12} \\ & - 3736a^{11} - 3116a^{10} + 620a^9 + 2112a^8 + 2104a^7 \\ & - 3924a^6 + 380a^5 + 328a^4 + 540a^3 - 16a^2 \\ & - 128a + 16\big)a^3x \\ & + a^{24} - 24a^{23} + 238a^{22} - 1236a^{21} + 3404a^{20} \\ & - 3672a^{19} - 4088a^{18} + 13880a^{17} - 5156a^{16} \\ & - 14376a^{15} + 10740a^{14} + 1944a^{13} + 6112a^{12} \\ & - 8144a^{11} - 4776a^{10} + 5168a^9 + 16a^8 - 112a^7 \\ & + 464a^6 - 512a^5 + 480a^4 - 352a^3 + 48a^2 - 32a \\ & + 16. \end{aligned} \tag{A.1}$$

Table 3
Coefficients h_i of Eq. (A.2), defining all 12 chiral period-8 orbits for $a = 6$

i	h_i	h_{25+i}
0	4081915149653776	697379517174320
1	11825088143620608	−87381313486024
2	−21887282277722272	−118322373946016
3	−82322190795741696	16824678098308
4	48659701836748656	16591507043024
5	260604190051529856	−2615779402208
6	−57644966578548320	−1915768060896
7	−501527340806731008	329089897596
8	38106168440918880	180911917240
9	661197366740943936	−33409481984
10	−12909016244098816	−13821145376
11	−637192640245999552	2715269920
12	2955979290938928	840409988
13	467335987309604848	−174177728
14	−4789407335604992	−39694696
15	−268058220368684576	8620548
16	6896813076468784	1402860
17	122590329613695440	−317488
18	−5574109992989408	−34884
19	−45330203043210448	8190
20	3013920528548744	544
21	13689755360380576	−132
22	−1194224609938768	−4
23	−3400036376577488	1
24	363628094999840	

Table 4
Orbital points for the chiral doublets of Fig. 4, roots of Eq. (A.2). The $(x_t, y_t) = (x_t, x_{t-1})$ values generate the leftmost partner in the first column. The conjugate orbit is obtained iterating (y_t, x_t)

Partners	σ	x_t	y_t
11 & 13	−5.2990	2.557920295	2.087622867
19 & 25	−4.8897	2.486117961	2.434927209
23 & 29	−0.0059	0.904220716	2.415258053
43 & 53	4.0444	2.506137179	2.132958329
55 & 59	4.8119	0.866194464	2.507859588
47 & 61	5.3383	1.346844933	1.534072957

These coefficients are the key to the divisibility of individual orbits. The complete polynomial requires about two extra pages to be recorded and is therefore omitted. It is however available from the authors on request. We just mention that this and similar polynomials for higher periods represent parameterized functions having cyclic Galois group and an exceptionally high degree of symmetries and invariances.

Table 4 indicates for $a = 6$ the proper in-phase sequence of roots needed to iterate Eq. (1) and obtain the orbits in Fig. 4. The 12 period-8 orbits are defined by the roots of

$$\mathbf{W}_8(x) = \sum_{i=0}^{48} h_i x^i, \tag{A.2}$$

with h_i being listed in Table 3 and pairs of roots in Table 4.

References

[1] M. Hénon, Celestial Mech. Dyn. Systems 93 (2005) 87.
[2] G. Voyatzis, J.D. Hadjidemetriou, Celestial Mech. Dyn. Systems 93 (2005) 263.
[3] S. Bolotin, Celestial Mech. Dyn. Systems 93 (2005) 343.
[4] S. Ferraz-Mello, T. Michtchenko, C. Beaugé, Astrophys. J. 621 (2005) 473.
[5] Y. Yamaguchi, K. Tanikawa, Prog. Theor. Phys. 113 (2005) 935; Y. Yamaguchi, K. Tanikawa, Prog. Theor. Phys. 114 (2005) 763.
[6] J. Schneider, T. Tél, Z. Neufeld, Phys. Rev. E 66 (2002) 066218.
[7] J.D. Meiss, Rev. Mod. Phys. 64 (1992) 795.
[8] G. Gibson, C. Jeffries, Phys. Rev. A 29 (1984) 811.
[9] D.G. Sterling, H.R. Dullin, J.D. Meiss, Physica D 134 (1999) 153.
[10] A. Endler, J.A.C. Gallas, Phys. Rev. E 65 (2002) 036231.
[11] A. Endler, J.A.C. Gallas, Physica A 344 (2004) 491.
[12] A. Endler, J.A.C. Gallas, Phys. Lett. A 352 (2006) 124; A. Endler, J.A.C. Gallas, C. R. Acad. Sci. (Paris) Ser. I 342 (2006) 681.
[13] J.A.C. Gallas, Physica A 283 (2001) 17.
[14] K.Th. Vahlen, in: Encyklopädie der mathematischen Wissenschaften, vol. I, Teubner, Leipzig, 1898–1904, pp. 449–479, paper I B3b.
[15] G.E. Andrews, Number Theory, Dover, New York, 1994, Section 6-4, reprint of the 1971 original.
[16] J.A.G. Roberts, F. Vivaldi, Nonlinearity 18 (2005) 2171.
[17] H. Poincaré, Méthodes Nouvelles de la Mécanique Céleste, Gauthier–Villars, Paris, 1892–1899, 3 volumes.
[18] G.D. Birkhoff, Trans. Am. Math. Soc. 18 (1917) 199.
[19] G.D. Birkhoff, Dynamical Systems, American Mathematical Society, New York, 1927.
[20] R. de Vogelaere, in: S. Lefschetz (Ed.), Contributions to the Theory of Nonlinear Oscillations, vol. IV, in: Ann. Math. Studies, vol. 41, Princeton Univ. Press, Princeton, 1958.
[21] R.L. Devaney, Trans. Am. Math. Soc. 218 (1976) 89.
[22] E. Piña, L. Jiménez Lara, Physica D 26 (1987) 369.
[23] L. Jiménez Lara, E. Piña, Celestial Mech. Dyn. Systems 49 (1990) 327.

[24] J.S.W. Lamb, J.A.G. Roberts, Physica D 112 (1998) 1.
[25] C. Störmer, The Polar Aurora, Oxford Univ. Press, Oxford, 1955.
[26] C. Mira, Chaotic Dynamics—From One-Dimensional Endomorphism to Two-Dimensional Diffeomorphism, World Scientific, Singapore, 1987.
[27] H. Kawakami, C. R. Acad. Sci. (Paris) Ser. I 301 (1985) 643.
[28] H. Kawakami, in: G. Ikegami (Ed.), Dynamical Systems and Nonlinear Oscillations, World Scientific, Singapore, 1986, pp. 73–92.
[29] A. Endler, J.A.C. Gallas, Orbital reversibility and conjugacy classes in a Hamiltonian repeller, preprint.
[30] S. Friedland, J. Milnor, Ergodic Theory Dynamical Systems 9 (1989) 67.
[31] E.F. Manffra, H. Kantz, W. Just, Phys. Rev. E 63 (2001) 46203.
[32] Y. Hirata, A.I. Mees, Phys. Rev. E 67 (2003) 26205.
[33] Y. Hirata, K. Judd, D. Kilmister, Phys. Rev. E 70 (2004) 16215.